35th Annual International Conference of the IEEE EMBS
Osaka, Japan, 3 - 7 July, 2013

An Automatic Bone Segmentation Method

Based on Anatomical Structure for the Knee Joint in MDCT Image

Y. Uozumi, and K. Nagamune, *Member, IEEE*

Abstract— **The purpose of this study is to propose an automatic segmentation about each bone (the femur, the tibia, the patellar, and fibular) of the knee in MDCT image. The proposed method was applied for six patients (Age 33 ± 13, four males / tew females). The proposed method segmented the knee joint into each bone by using anatomical structure for the knee joint. The experiments calculate matching rate of the manual and the proposed method for evaluating it. As a result, The matching rate of the femur, the tibia, the patellar, and fibula were 95.84 ± 0.57 %, 94.12 ± 1.01 %, 94.49 ± 0.83 %, 86.37 ± 4.28 %, respectively. This study concluded that the proposed method is enough to segment the knee bones.**

I. Introduction

It is significant to analyze the bone shape of the knee joint, because the knee kinematics are clearly influenced by bony morphology. Variation of femoral condyle morphology has been associated with a risk of anterior cruciate ligament (ACL) injury [1] and is a factor for proper fitting of total knee arthroplasty (TKA) implants [2]. Knee kinematics varies considerably between individuals during in vivo dynamic activity [3], and it is reasonable to suggest that bony morphology might influence knee motion. However, it is relatively unknown about effect of anatomic variation of the femur to knee kinematics.

The rapid advancement of diagnostic technique with medical imaging has contributed to the effective diagnosis and treatment of numerous diseases from appendicitis to brain cancer [4]. The advancement of image analysis as a major factor in medical decision making has directly led to a drive towards quantification of image findings, in order to examine the mostly visual evaluation of trained medical professionals. Segmentation of computed tomography (CT) and magnetic resonance (MR) scan data has become the accepted standard for subject-specific model development [5]. However, the processing is typically manual and time-consuming. For instance, extracting the articular surfaces of a knee joint was reported as requiring approximately two days of work [5]. Recent studies have investigated various aspects of automating the extraction process. Automated threshold-based algorithms have been employed to extract bones from CT scans [6]. The problems of past studies take a great deal of effort. In addition, since this results have large variation, past studies has been not objective evaluation. Therefore, the extraction and segmentation are desired to be automatic to solve the problems and disadvantages by manual method.

It is important to segment the each bone (the femur, the tibia, the patellar, and fibular) for much analysis methods. The purpose of this study is to propose an automatic extraction and segmentation of the knee bones with a segmentation method in MDCT image.

Methods

This method consists of three steps to segment the knee bones. First step is to segment the femur and tibia. Second step is to segment the femur and patellar. Final step is to segment the tibia and fibular.

A. Segmentation Between the Femur and Tibia

This step determines border slice of the femur and tibia, and classifies the femur and tibia. This process determines the slice between the femur and tibia, using a scatter graph of intensity. The intensity in MDCT images uses a unit of HU. In top image of Fig. 1, search slice indicates border between the femur and tibia. The knee MDCT image has the slice range from proximal the femur (slice 0) to distal the tibia (slice 200). A central image of Fig. 1 is a axial plane on the femur and patellar. The intensity of the cortical bone, cancellous bone, soft tissue locate about 2000, 500, and 100, respectively. The bottom image of Fig. 1 is scatter graph of intensity. Slices about 0-100 and 100-200 can be regarded as the femur and tibia region. A turning point of slice about 100 indicates border between the femur and tibia, respectively. This process calculates a turning point of the scatter graph of intensity in order to determine the boundary between the femur and tibia. An evaluation graph for the femur-tibia border is calculated based on a degree. The evaluation value of the intensity distribution $\mu_{if}(s)$ is calculated from

$$\begin{cases} \mu_i(s) = 1 - \dfrac{1}{I} i(s) \\ \mu_f(s) = 1 - \dfrac{1}{F} f(s) \end{cases} \tag{1}$$

$$\mu_{if}(s) = \mu_i(s) \times \mu_f(s) \tag{2}$$

where s is the number of slice. $\mu_i(s)$ and $\mu_f(s)$ are the membership functions for the intensity and the frequency, respectively. i and f are the intensity and the frequency, respectively. I and F are the maximum of the intensity and the frequency, and are set to be 2500 and 4 in this study,

Y. Uozumi is with Graduate School of Engineering, University of Fukui, Fukui, Japan (e-mail: uozumi@me.his.u-fukui.ac.jp).

K. Nagamune is with Graduate School of Engineering, University of Fukui, Fukui, Japan (corresponding author to provide phone: +81-776-27-8037; fax: +81-776-27-8037; e-mail: nagamune@me.his.u-fukui.ac.jp).

respectively. The evaluation graph is recalculated as differential of the frequency. Then, the local maximum of the border slice between the femur and tibia is detected. The local maximum of the border slice s_{max} is calculated from

$$s_{\max} = \arg\max_{s}\left(\mu_{if}(s) - \frac{1}{N-1}\left(\int_{j} \mu_{if}(j)dj + \int_{k} \mu_{if}(k)dk \right) \right) \quad (3)$$

where $j \in [s-1, s-N/2]$ and $k \in [s+1, s+N/2]$ are the numbers of differential ranges, respectively. N is the size of differential range, and is set to be 5 in this study. The femur and tibia are segmented by the border slice s_{max}.

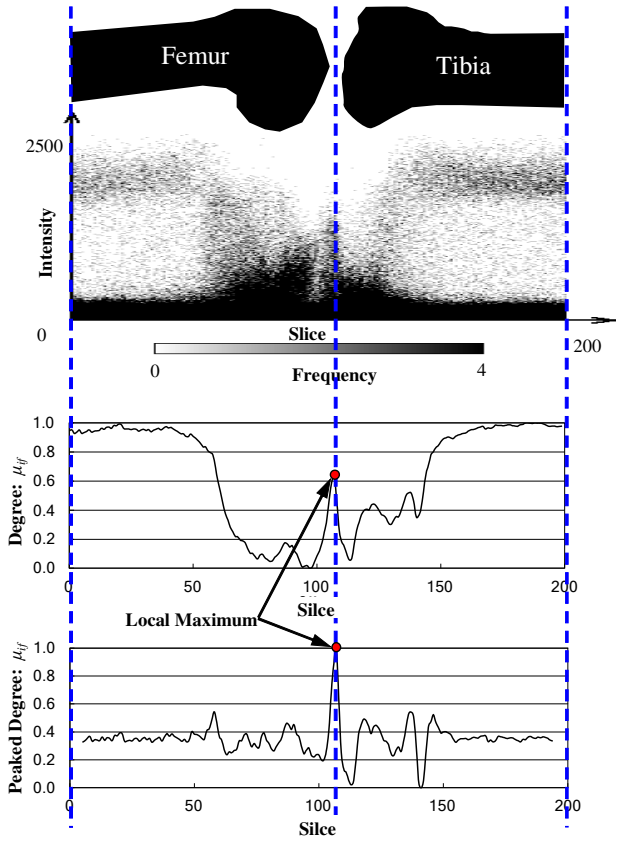

Figure 1. Graph of intensity distribution. Upper image is axial plane on the femur and patellar. Intensity of cortical bone , cancellous bone, soft tissue locate about 2000, 500, and 100, respectively. Center image is graph of the intensity distribution. Slice about 0-100 and 100-200 are the femur and tibia region. Turning point of slice about 100 indicates border between the femur and tibia. In evaluation graph, local maximum point (shape of impulse) about slice 100 is border slice between the femur and tibia. Under image is determination of border slice between the femur and tibia in differential.

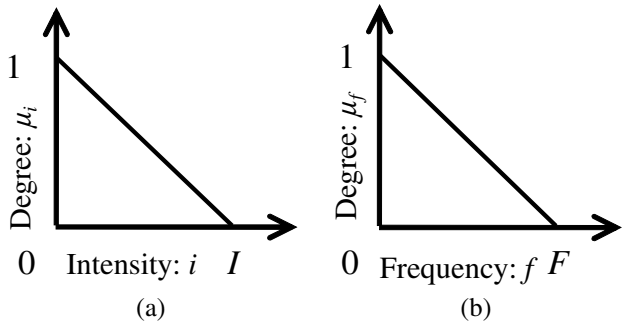

Figure 2. Membership function for (a) intensity and (b) frequency.

B. Segmentation Between the Femur and Patellar

This step classifies the femur and patellar. This method has the stream from the raw (Fig. 3(a)) to the binarization (Fig. 3(b)), the closing (Fig. 3(c)), and the extraction (Fig. 3(d)). Since the intensity of border between the soft tissue and the bone (cancellous and cortical bone) region in the raw MDCT image has fuzzy distribution (Fig. 3(a)), to set the threshold of the binarization by manual is difficult, has not quantitative, and has take a lot of hard works. Therefore, it is important to binarize the raw image using the accurate and automatic threshold. If threshold is too small and large, it is impossible to segment the femur and patellar. This process secondary differentiates the intensity-frequency graph, detects the maximum value of the threshold to segment the femur and patellar dynamically. Fig. 4(a) indicates the frequency (number) of the intensity for the object pixel, and has the intensity between the soft tissue and bone about 300. Fig. 4(b) indicates the secondary differentiation for the intensity to frequency, and determines the threshold of the intensity between the soft tissue and bone about 300. The second differential $T'(t)$ is calculated from

$$T'(t) = \frac{d^2}{dt^2} T(t) \quad (4)$$

where t and $T(t)$ are the intensity and the frequency of the intensity, respectively. The process of binarization makes the threshold to set the maximum value of $T'(t)$ (local maximum of Fig. 4(b)), and binarize the raw image to the binarized image.

Since the binarized image has the void region within the binarized pixel (pixel at bone), the process of the closing fill the void region (Fig. 3(c)). The process of extraction extracts from the closed image to the region of the femur or the patellar bone (Fig. 3(d)).

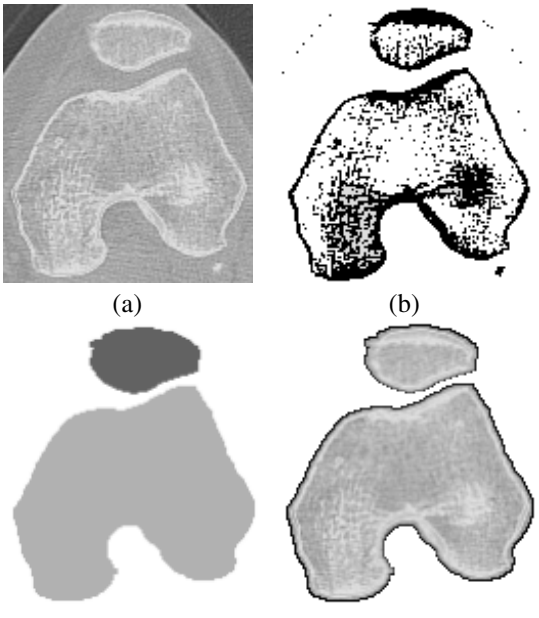

Figure 3. Flowchart of segmentation between the femur and patellar in (a) raw, (b) binarization, (c) closing, and (d) extraction.

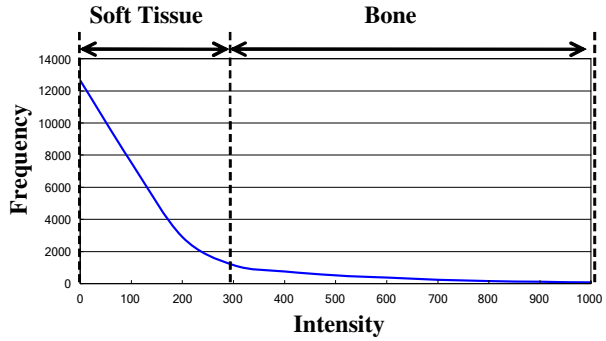

(a)

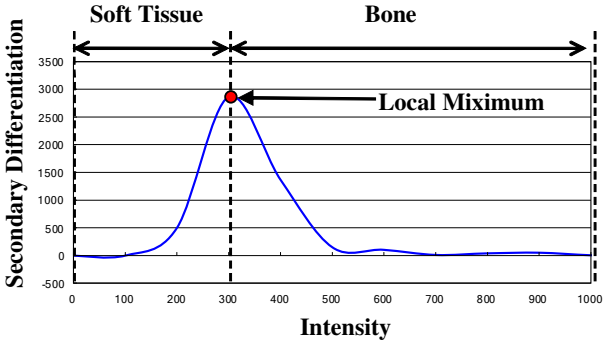

(b)

Figure 4. Dynamic threshold to segment the femur and patellar. (a) Frequency indicates the number of the intensity for the object pixel, and has the intensity between the soft tissue and bone about 300. (b) Second differential indicates the secondary differentiation for the intensity to frequency, and determines the threshold of the intensity between the soft tissue and bone about 300.

C. *Segmentation Between the Tibia and Fibular*

This process makes the intensity distribution between the tibia and patellar (Fig. 5). A range is a distance between the tibia and fibular. In a intensity-range graph, the range about 55 % is the border between the tibia and fibular. This process emphasizes the local minimum by the degree, and determines local minimum of range between the tibia and fibular. The local minimum the border r_{mix} is calculated from

$$\mu_{tf}(r)=\begin{cases} 1-\dfrac{2}{R}r & (0\le r\le R/2) \\ -1+\dfrac{2}{R}r & (R/2<r\le R) \end{cases} \tag{5}$$

$$r_{min}=\arg\min_{r}\left(\mu_{tf}(r)\right) \tag{6}$$

where r is the number of range. R is the maximum value of range, is set to be 100 in this study (Fig. 6). μ_{tf} is the degree. The tibia and fibular are segmented by the local minimum r_{min}.

III. Experiments

The proposed method was applied to MDCT image data sets of six patients (Age 33 ± 13, four males / two females). Since this study is a pilot study, the number of sample sets to be six. An examiner visually evaluated the segmentation results of each bone. This experiments used matching rate that

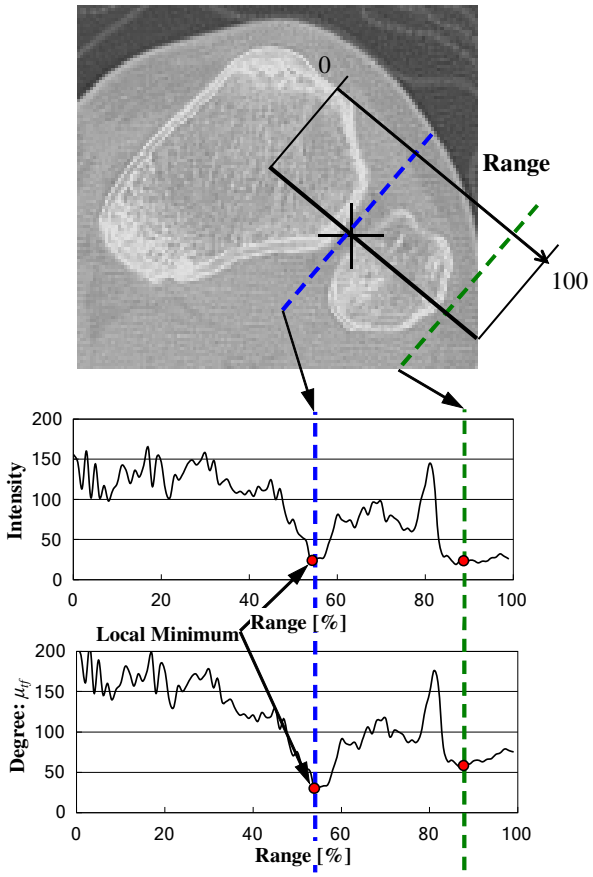

Figure 5. Flowchart of segmentation between the tibia and fibular. Border between the tibia and fibular locates range about 55 %.

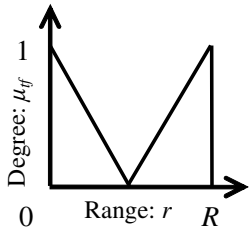

Figure 6. Membership function for range between the tibia and fibular.

compared the accuracies in the experimental results by the manual and proposed method. The matching rate M is calculated from

$$M=\frac{1}{2}\left(\frac{V_{\alpha\beta}}{V_{\alpha}}+\frac{V_{\alpha\beta}}{V_{\beta}}\right) \tag{7}$$

where α and β are the manual and proposed method data, respectively. V_{α} and V_{β} are the volumes of the binary images of α and β by a simple thresholding process, respectively. $V_{\alpha\beta}$ is the matching volume between V_{α} and V_{β}. A matching rate is a value calculated by dividing a twice volume of overlap region by a summation volume of both region. We dealt with this matching rate as accuracy.

This experiments analyzed the MDCT images. The acquisition parameters were as follows. The resolution on a slice was 512 × 512 (X × Y) voxels. The range of intensity was 16 bits. The thickness of slice was 1.0 mm. The total number of slice was 200. The range of image about z-axis was 50 mm

proximal from the femoral epicondyles and 50 mm distal from the tibial tubercles.

IV. Results

Fig. 7 shows the matching rate that compared the segmentation results by the manual and proposed method. The matching rate of the femur, the tibia, the patellar, and fibula were 95.84 ± 0.57 %, 94.12 ± 1.01 %, 94.49 ± 0.83 %, 86.37 ± 4.28 %, respectively. The results indicate that the proposed method could be segmented for all patients. Fig. 8 shows the segmented knee bones that are the femur, the tibia, the patellar, and fibular in the MDCT images.

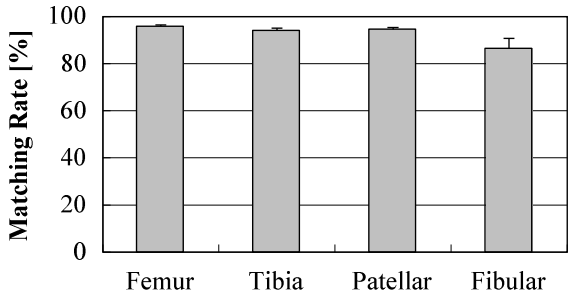

Figure 7. Matching rate for the compared segmentation results by the

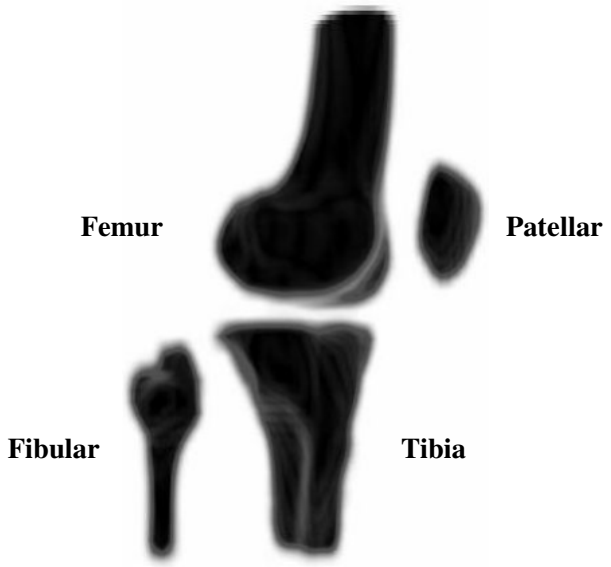

Figure 8. Segmented knee bones that are the femur, the tibia, the patellar, and the fibular.

V. Discussion

Matching rate of the manual and the proposed method shows high values (Fig. 7). Therefore, the proposed method was useful to extract and segment each bone in actual scene.

The manual extraction and segmentation of the knee bone shape have each problem and disadvantage such as the large burden, the long time, the subjective (not objective) evaluation, and not so high reproducibility. Our method could perform the automatic extraction and segmentation, solve those problems of manual method, and show three advantages. First, our method is to reduce the burden of the examiner, because it is full automatic extraction and segmentation. Second, computation time of the proposed method indicates shorter than manual method. Although the manual method of the extraction and segmentation process needs almost one day per subject, the proposed method executed the extraction and segmentation process within about five minute per subject with PC (Intel(R), Core(TM), i7 CPU, 920 @ 2.67 GHz, 9.99 GM RAM). Third, our method could objectively segment and extract the bones, because the process is executed based on one algorithm. Fouth, the proposed method has high reproducibility, because it performs to make quite same results from same data.

Ramme et al. [7] reported that bone segmentation for the knee joint in CT image. Although their accuracies in the experimental results were 98%(femur) and 98%(tibia), the study extracted only the femur and tibia. Our proposed method extracted all the knee joint bone (the femur, the tibia, the patellar, and the fibular). Therefore our proposed method could be able to analyze clinical data.

VI. Conclusion

This study proposed an automatic segmentation method with anatomical structure for the bones of the knee in MDCT image. In the results, the proposed method was high precision to extract and segment each bone. This study concluded that our method is enough to segment each bone in the MDCT images. This study indicated that our proposed method can contribute to analyze clinical data.

Acknowledgment

Authors would like to thank Prof. M. Kurosaka and Associ. Prof. R. Kuroda of Kobe University Graduate School of Medicine for providing the MDCT data and giving good comments.

References

[1] T. E. Hewett, G. D. Myer, K. R. Ford, "Anterior cruciate ligament injuries in female athletes: part 1, mechanisms and risk factors," Am J Sports Med, Vol. 34, pp. 299-311, 2006.

[2] J. H. Lonner, J. G. Jasko, B. S. Thomas, "Anthropomorphic differences between the distal femora of men and women," Clin Orthop Relat Res, Vol. 466, pp. 2724-2729, 2008.

[3] S. Tashman, P. Kolowich, D. Collon, K. Anderson, W. Anderst, "Dynamic function of the ACL-reconstructed knee during running," Clin Orthop Relat Res, Vol. 454, pp. 66-73, 2007.

[4] W. E. Brant, C. A. Holms, "Fundamentals of Diagnostic Radiology," third ed. Lippincott Williams & Wilkins, Philadelphia, PA, 2006.

[5] Z. A. Cohen, D. M. McCarthy, S. D. Kwak, P. Legrand, F. Fogarasi, E. J. Ciaccio, G. A. Ateshian, "Knee cartilage topography, thickness, and contact areas from MRI: in-vitro calibration and in-vivo measurements," Osteoarthritis and Cartilage, Vol. 7, pp. 95-109, 1999.

[6] F. Taddei, L. Cristofolini, S. Martelli, H. S. Gill, M. Viceconti, "Subject-specific finite element models of long bones: an in vitro evaluation of the overall accuracy," Journal of Biomechanics, Vol. 39, pp. 2457-2467, 2006.

[7] A. J. Ramme, A. J. Criswell, B. R. Wolf, V. A. Magnotta, N. M. Grosland, "EM segmentation of the distal femur and proximal tibia: a high-throughput approach to anatomic surface generation," Annals of Biomedical Engineering Vol. 39, pp. 1555-1562, 2011.